Report

Higher plant photosynthetic capability in autumn responding to low atmospheric vapor pressure deficit

Yawen Wang,[1] Wenfang Xu,[2] Wenping Yuan,[2,*] Xiuzhi Chen,[2] Bingwei Zhang,[3] Lei Fan,[4] Bin He,[5] Zhongmin Hu,[6] Shuguang Liu,[7] Wei Liu,[8] and Shilong Piao[9]

*Correspondence: yuanwp3@mail.sysu.edu.cn

Received: January 22, 2021; Accepted: September 2, 2021; Published Online: September 7, 2021; https://doi.org/10.1016/j.xinn.2021.100163

Graphical abstract

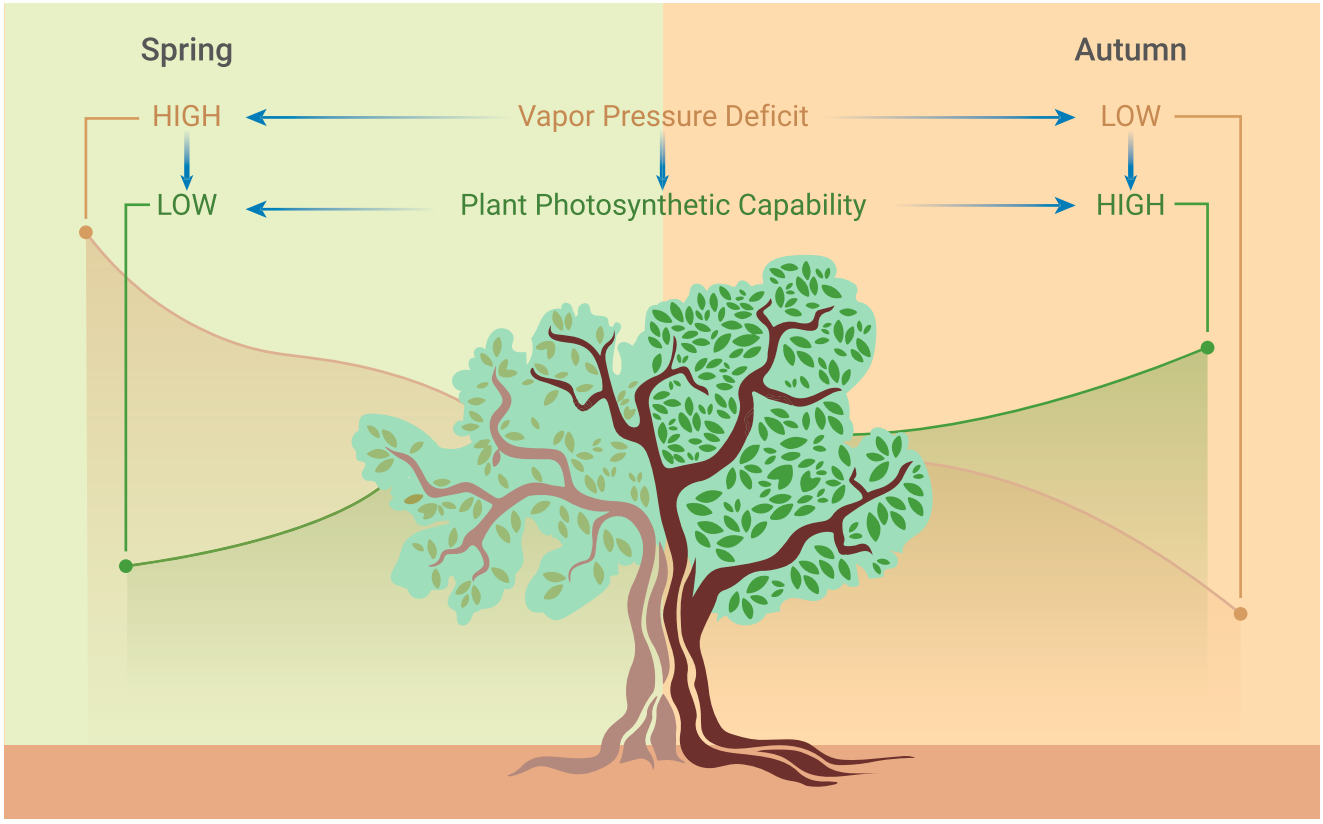

Public summary

- Autumn VPD is lower than spring VPD at the same air temperature over majority of the extratropical vegetated land
- Photosynthetic capability is significantly higher in autumn than in spring due to lower VPD
- Earth System Models projected continuous larger VPD values in spring as against autumn

Report

Higher plant photosynthetic capability in autumn responding to low atmospheric vapor pressure deficit

Yawen Wang,[1] Wenfang Xu,[2] Wenping Yuan,[2,*] Xiuzhi Chen,[2] Bingwei Zhang,[3] Lei Fan,[4] Bin He,[5] Zhongmin Hu,[6] Shuguang Liu,[7] Wei Liu,[8] and Shilong Piao[9]

[1]Physical Oceanography Laboratory, College of Oceanic and Atmospheric Sciences, Ocean University of China, Qingdao 266100, China
[2]School of Atmospheric Sciences, Southern Marine Science and Engineering Guangdong Laboratory (Zhuhai), Sun Yat-sen University, Zhuhai 519082, China
[3]Zhuhai Branch of State Key Laboratory of Earth Surface Processes and Resource Ecology, Beijing Normal University at Zhuhai, Zhuhai 519087, China
[4]School of Geographical Sciences, Nanjing University of Information Science and Technology, Nanjing 210044, China
[5]College of Global Change and Earth System Science, Beijing Normal University, Beijing 100038, China
[6]School of Geography, South China Normal University, Guangzhou 510631, China
[7]National Engineering Laboratory for Applied Technology of Forestry & Ecology in South China and College of Biological Science and Technology, Central South University of Forestry and Technology, Changsha 410004, China
[8]State Key Laboratory of Vegetation and Environmental Change, Institute of Botany, Chinese Academy of Sciences, Beijing 100093, China
[9]Sino-French Institute for Earth System Science, College of Urban and Environmental Sciences, Peking University, Beijing 100871, China
*Correspondence: yuanwp3@mail.sysu.edu.cn

Received: January 22, 2021; Accepted: September 2, 2021; Published Online: September 7, 2021; https://doi.org/10.1016/j.xinn.2021.100163

Citation: Wang Y., Xu W., Yuan W., et al., (2021). Higher plant photosynthetic capability in autumn responding to low atmospheric vapor pressure deficit. The Innovation **2(4)**, 100163.

It has been long established that the terrestrial vegetation in spring has stronger photosynthetic capability than in autumn. However, this study challenges this consensus by comparing photosynthetic capability of terrestrial vegetation between the spring and autumn seasons based on measurements of 100 *in situ* eddy covariance towers over global extratropical ecosystems. At the majority of these sites, photosynthetic capability, indicated by light use efficiency (LUE) and apparent quantum efficiency, is significantly higher in autumn than in spring, due to lower atmosphere vapor pressure deficit (VPD) at the same air temperature. Seasonal VPD differences also substantially explain the interannual variability of the differences in photosynthetic capability between spring and autumn. We further reveal that VPD in autumn is significantly lower than in spring over 74.14% of extratropical areas, based on a global climate dataset. In contrast, LUE derived from a data-driven vegetation production dataset is significantly higher in autumn in over 61.02% of extratropical vegetated areas. Six Earth system models consistently projected continuous larger VPD values in spring compared with autumn, which implies that the impacts on vegetation growth will long exist and should be adequately considered when assessing the seasonal responses of terrestrial ecosystems to future climate conditions.

Keywords: light use efficiency; vapor pressure deficit; vegetation index; carbon cycle

INTRODUCTION

As one fundamental and important characteristic of terrestrial ecosystems, seasonal dynamics of vegetation growth plays an important role in regulating the temporal changes of terrestrial carbon budget and atmospheric CO_2 concentrations.[1–3] It has been long deemed that the vegetation production in spring responds more positively to climate warming and is higher than in autumn at the same air temperature, since solar radiation is usually not a limiting factor in spring (Figures S1 and S2).[4–6] Previous evidence led to a conclusion that vegetation growth in spring plays a more important role for the terrestrial carbon sink than in autumn.[7,8] Although the mechanisms behind this remain unclear, several recent studies challenged this conclusion by proposing a comparable or even larger contribution of the vegetation growth in autumn to vegetation production throughout the entire year.[9–11] For example, the mean increases of vegetation production per day of later autumn were observed to be larger than that of earlier spring over the eastern United States.[12]

An important cause of the complicated seasonal dynamics of vegetation growth is that other factors besides air temperature and solar radiation may influence vegetation growth. Air temperature is one of the most important extrinsic factors regulating vegetation growth across the diurnal, seasonal, and annual scales.[13] Numerous studies have shown substantial impacts of air temperature on plant phenophases[14] and photosynthetic capability.[15] In addition, solar radiation has traditionally been considered as the determining factor for vegetation growth because photosynthesis is a process of converting solar energy into chemical energy.[16] Besides air temperature and solar radiation, recent studies have increasingly proposed atmospheric vapor pressure deficit (VPD), i.e., the difference between the water vapor pressure at saturation and the actual water vapor pressure for a given air temperature, as one important driver of global terrestrial vegetation growth.[17,18] VPD increases with rising air temperature because the actual atmospheric water vapor content does not increase by the same amount as the exponential increase in saturated vapor pressure.[19] There are numerous knowledge gaps concerning the impacts of VPD on vegetation growth.[19] In particular, air temperature increases faster in spring and winter than in other seasons.[20] The non-uniform seasonal rates of climate warming may underpin the seasonal differences in atmospheric VPD and thereby proffer inconsistent impacts on vegetation growth during the two seasonal periods. However, the large-scale constraints of the seasonality of VPD on vegetation growth have not yet been quantified.

Through analyzing the seasonal dynamics of photosynthetic capability based on two indicators, namely light use efficiency (LUE) and apparent quantum efficiency, over 100 extratropical ecosystems globally using eddy covariance measurements, this study aims to (1) investigate the impacts of seasonal differences in VPD on the vegetation photosynthetic capability, (2) determine the global patterns and changes of the seasonal dynamics of VPD through an observation-based global climate dataset, and (3) quantify the impacts of seasonal differences in VPD on the global patterns of vegetation photosynthetic capability.

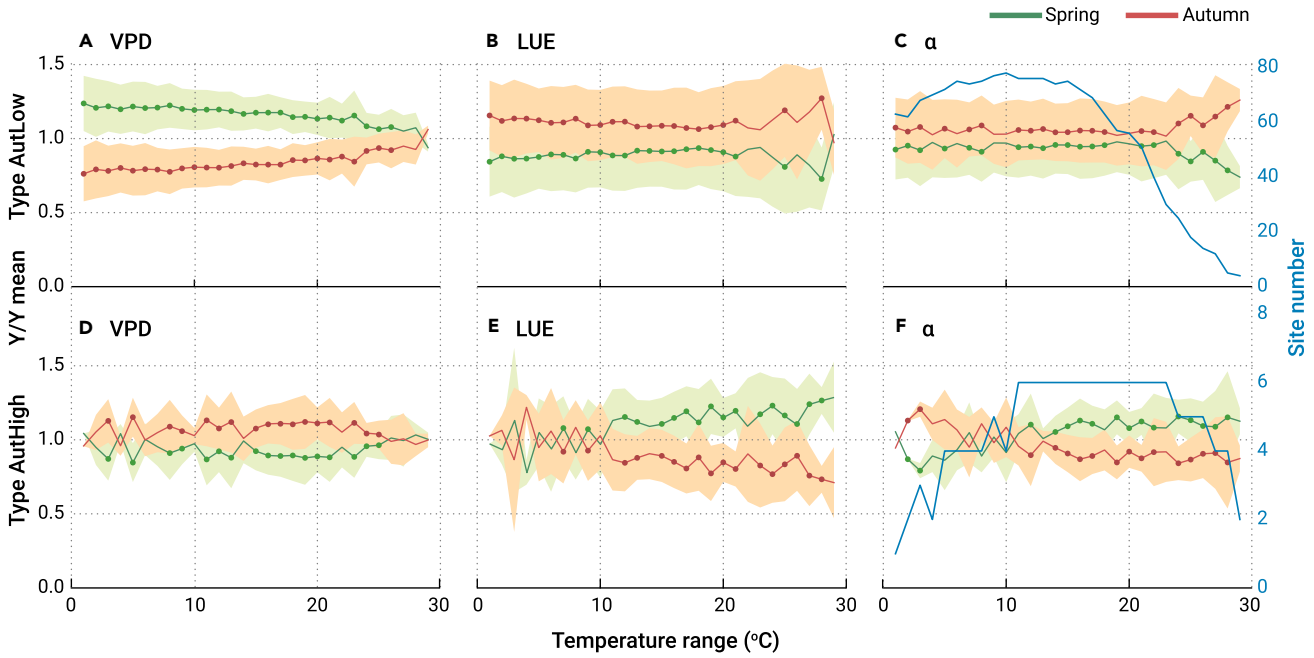

Figure 1. Comparisons of vapor pressure deficit (VPD) and two photosynthetic parameters (light use efficiency, LUE; apparent quantum efficiency, α) between spring and autumn for the AutLow and AutHigh types of sites (A–C) Comparisons of spring and autumn Y/Y_{mean} of the variables (see materials and methods) in different temperature ranges from 0°C to 29°C (the maximum air temperature of the spring and autumn seasons) at 1°C intervals averaged over the 80 AutLow sites. (D–F) Same as (A) to (C) averaged over the six AutHigh sites. The green and red lines indicate spring and autumn Y/Y_{mean}, respectively, with the shadow indicating the corresponding standard deviations. Dots in the lines denote significant ($p < 0.05$) differences in Y/Y_{mean} between spring and autumn. Blue lines in (C) and (F) show the site number for each temperature range.

RESULTS

The measurements and estimates at all 100 eddy covariance towers reveal distinct differences in VPD and the photosynthetic capability between spring and autumn. At 80 out of the total 100 sites (80%), VPD at the same air temperature is significantly lower in autumn than in spring (referred to as type AutLow), implying a lower atmospheric water demand in autumn (Figures S4, S5A, S5B, and 1A). Through all the type AutLow sites, the averaged LUE and apparent quantum efficiency (α) are significantly higher in autumn than in spring at most temperature ranges (Figures 1B and 1C), indicating a stronger photosynthetic capability in autumn. Specifically, LUE and α are significantly higher in autumn than in spring over 65% and 46.25% of the type AutLow sites, respectively, and only 15% and 18% of sites respectively show significantly lower values (Figure 2; see materials and methods). In contrast, six sites show significantly higher VPD in autumn (referred to as type AutHigh) (Figures S4, S5C, S5D, and 1D), while the remaining 14 sites show insignificant differences in spring and autumn VPD (Figure S4). The averaged LUE and α over the six type AutHigh sites in autumn are significantly lower than in spring at most temperature ranges (Figures 1E and 1F) and sites (Figure 3).

We further investigated the correlations between VPD and the two photosynthetic parameters (LUE and α) on a monthly basis. Significantly negative correlations were found over most sites (see red lines in Figure S6), indicating strong inhibitions of VPD on the photosynthetic capability. Besides, throughout the type AutLow sites, the percentages of significantly negative correlations between VPD and two parameters in the autumn months (September to November) were generally lower than in the spring months (March to May) (Figures S6A and S6B), which implies weaker constraints of VPD to photosynthesis in autumn due to lower VPD. In contrast, there were higher percentages of significantly negative correlations in autumn over the type AutHigh sites, coinciding with higher autumn VPD at these sites (Figures S6C and S6D).

In addition, we also examined the role of VPD in influencing the interannual variability of the seasonal differences in photosynthetic capability at 25 eddy covariance sites with more than 10 years of continuous measurements (Table S1). The interannual variability of the differences between spring and autumn VPD are significantly and negatively correlated with the seasonal differences in LUE and α over 68% and 48% of the 25 sites, respectively. Significantly positive correlations were found only over one site for LUE and over no site for α (Figure 4).

Based on an observation-based globally gridded climate dataset (Climatic Research Unit [CRU]), we analyzed the global pattern of the seasonal dynamics of VPD. Similar to the findings from eddy covariance sites, autumn VPD is significantly lower than spring VPD at the same air temperature over nearly 74.14% of the extratropical vegetated land (Figure 5), i.e., type AutLow, suggesting a lower atmospheric water demand. In contrast, only 12.12% of extratropical vegetated land, mainly distributed over southern China, northeastern America, and central Asia, shows significantly larger autumn VPD than spring VPD (i.e., type AutHigh) (Figure 5).

Contrary to lower VPD in autumn indicated by the CRU dataset over most of the extratropical land, LUE derived from data-driven gross primary productivity (GPP) datasets (Max Planck Institute for Biogeochemistry [MPI-BGC] GPP[21]) for 1982–2015 are significantly higher in autumn than at the same air temperature in spring over 61.02% of the extratropical vegetated areas (Figure 6). In contrast, 16.19% of areas shows significantly lower LUE in autumn (Figure 6), largely distributed over the type AutHigh areas with higher autumn VPD (Figure 5). In addition, it is noteworthy that both VPD and LUE are lower in autumn than in spring over northern China, Europe, and central America. These regions typically comprise fields of winter wheat, with spring as the main growing season for winter wheat, which in turn leads to higher LUE in spring.

DISCUSSION

Our results suggest higher photosynthetic capability of terrestrial vegetation in autumn than at the same air temperature in spring over the majority of extratropical land, which challenges previous consensus of a higher photosynthetic capability in spring.[7] Lower atmospheric water demand plays an important role in determining higher photosynthetic capability in autumn than in spring (Figure 1). The differences in soil moisture between spring and autumn cannot explain the seasonal heterogeneity of photosynthetic

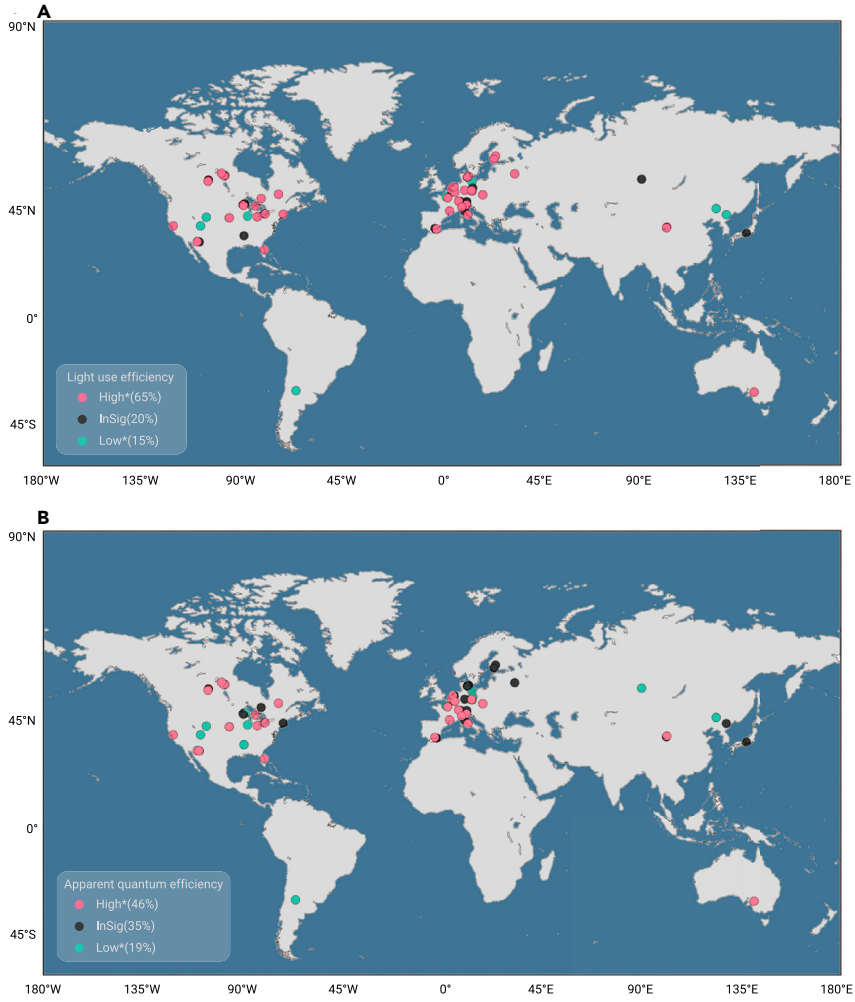

Figure 2. Differences in light use efficiency and apparent quantum efficiency in AutLow sites Differences in (A) light use efficiency and (B) apparent quantum efficiency between autumn and spring over the 80 AutLow sites with significantly lower vapor pressure deficit in autumn than in spring. High* and Low* indicate significantly higher and lower values of the two photosynthetic capabilities in autumn than in spring ($p < 0.05$), respectively. Insig indicates insignificant differences of the parameters between spring and autumn. Insets show the frequency distributions of the High*, Low*, and Insig types of sites.

capability (Figure S7). More than 72.02% (40.98% significant) of extratropical vegetated area shows lower soil moisture in autumn, which is not consistent with the global pattern of photosynthetic capability (Figure 6). In addition, the seasonal changes of atmospheric CO_2 concentration also potentially impact the differences in photosynthetic capability between spring and autumn.[22] However, the atmospheric CO_2 concentration in autumn is lower than that in spring (Figure S8), which cannot explain the higher photosynthetic capability in autumn (Figure 6). Other lines of evidence support our conclusion that an increase in VPD typically induces a decrease in steady-state stomatal aperture and stomatal conductance,[23,24] and eventually limits photosynthetic capability, which may be independently decreased by declining soil moisture and non-stomatal limitations to biochemical capacity.[25,26]

The lagged effects of air temperature on atmospheric water vapor constitute an important cause of lower VPD in autumn than in spring. The high air temperature and vegetation growth in summer benefits land evapotranspiration, which in turn leads to higher actual water vapor of the atmosphere in autumn than in spring.[27] Exceptions are found in limited regions with unique climate circulation, e.g., southern China, central Asia, and northeastern America (Figure 5). For example, in spring and early summer, the relatively warm and moist air mass from the Pacific and South China Sea encounters the cool continental air mass over southern China, resulting in a quasi-stationary front with prevailing rainfall and humid surface.[28]

Our results provide direct evidence for larger responses of vegetation growth in autumn as suggested in recent studies.[10,11] Huang et al.[10] noted that, at high latitudes, benefiting from climate warming, the northward displacement velocities of vegetation productivity in autumn are nearly twice those in spring during the period 1982–2011. The spring and autumn difference in VPD may have played an important role, and the impact has kept increasing during the present century and expectedly into the near future (Figure S9A). Due to the higher VPD increase in spring than in autumn (Figures S9B–S9E), the difference in VPD between spring and autumn significantly increases from 1901 to 2015 (Figure S9A), prevailing over 81.32% of the extratropical vegetated areas (significant over 44.03% of area) (Figure S10). The higher increase in saturated water vapor pressure than actual water vapor pressure in spring (Figure S11), as a result of a higher increase in air temperature in spring relative to other seasons,[20] has determined the enhanced spring and autumn VPD differences.

Six Earth system models participating in the Coupled Model Intercomparison Project Phase 5 (CMIP5) (Table S2) project a steady increase in spring and autumn VPD differences until the end of this century (Figure S9A). Our analysis suggests that the projected increasing VPD differences between spring and autumn might have a long-term impact on photosynthetic capability, and thus must be examined carefully when evaluating seasonal dynamics of the terrestrial carbon cycle. Moreover, solar radiation shows a larger increase in autumn than in spring (Figure S12), which will further enhance the differences in vegetation production between spring and autumn.

In this study, most of the investigated sites showed the spring and autumn differences in photosynthetic capability responding to the seasonal differences in VPD. However, there are contrary results at a few sites, e.g., 15% and 18% of sites for LUE and α, respectively, at AutLow sites (Figures 2 and 3). Variations in plant traits across species in response to VPD may be a major reason for the inconsistent conclusion.[29,30] Previous studies have represented the substantial variations in plant traits (e.g., vulnerability to xylem cavitation) across tree species and ecosystem types.[30] This difference

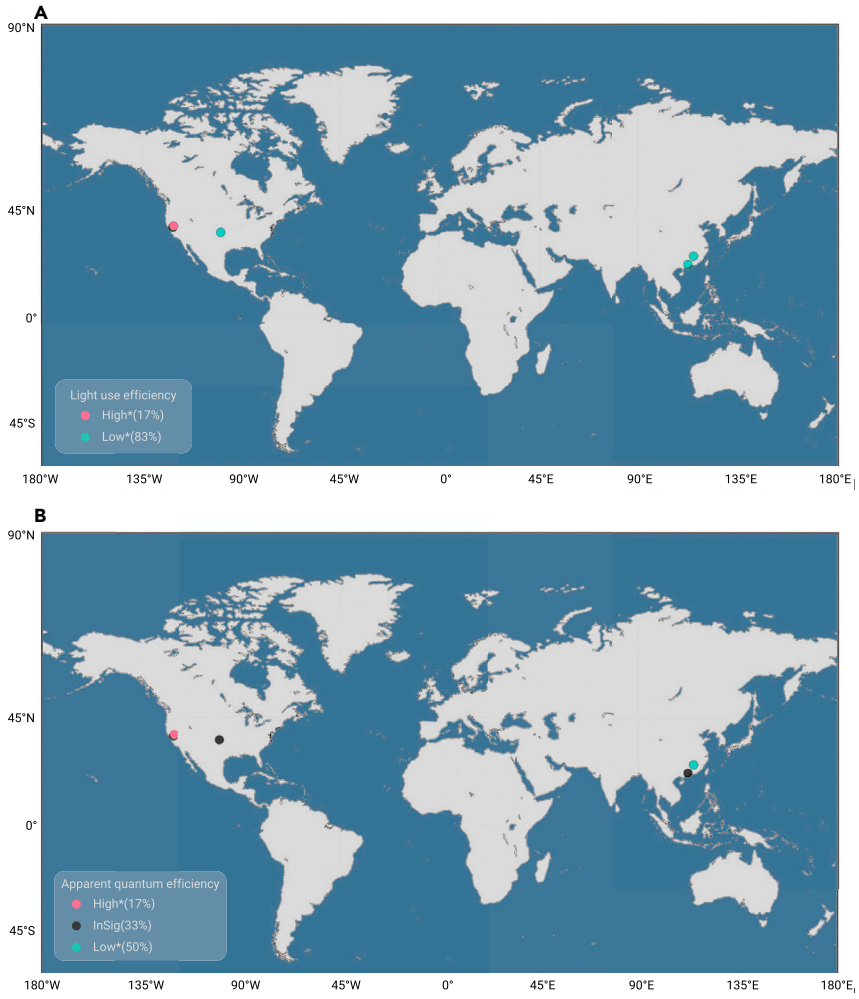

Figure 3. Differences in light use efficiency and apparent quantum efficiency in AutHigh sites Differences in (A) light use efficiency and (B) apparent quantum efficiency between spring and autumn at the same air temperature over the six AutHigh sites with higher vapor pressure deficit in autumn than in spring. High* and Low* indicate significantly higher and lower values in autumn than in spring ($p < 0.05$), respectively. Insig indicates insignificant differences of the parameters between spring and autumn. Insets show the frequency distributions of the High*, Low*, and Insig types of sites.

results from water-stress avoidance strategies that are used by some species, such as deep root systems or drought deciduousness, that allow them to maintain a higher xylem pressure during drier periods. Although the variability in plant hydraulic traits is well known, far fewer data are available to quantify within-species variation.[31] It is urgently necessary to investigate the differences in plant hydraulic traits among various plant species, especially for their responses to atmospheric VPD variations.[32] In addition, the responses, associated with plant traits, need to be incorporated into plant photosynthesis estimates to adequately assess the seasonal changes of the ecosystem production in response to climate change.

MATERIALS AND METHODS

Variables of photosynthetic capability

There are several commonly used indices for representing the photosynthetic capability such as LUE, α, and maximized photosynthetic rate. LUE and α are the two most common used indices because of their characteristics of simple calculation and high stabilization, and they exclude the impacts of radiation and thus indicate the internal photosynthetic capability of plants. Therefore, this study used LUE and α to indicate photosynthetic capability based on eddy covariance measurements from the FLUXNET2015 dataset: www.fluxdata.org (Table S1). We calculated the LUE (g C m^{-2} MJ^{-1}) as

$$LUE = \frac{GPP}{fPAR \times PAR}, \quad \text{(Equation 1)}$$

where GPP indicates the estimated gross primary production (g C m^{-2} MJ^{-1}), PAR is photosynthetically active radiation (MJ m^{-2}), and fPAR is the fraction of PAR absorbed by the vegetation canopy calculated by NASA's Global Inventory Modeling and Monitoring Study third-generation group (GIMMS3g) normalized difference vegetation index (NDVI).[33] We used SW × 0.45 as a substitute for PAR at the sites without PAR measurements, where SW is incoming shortwave radiation (MJ m^{-2}). GPP, PAR, and SW are all from the eddy covariance measurements. We used the linear interpolation method to generate daily fPAR values based on two adjacent half-monthly observations, and therefore LUE was calculated at daily scale.

The α (g C m^{-2} MJ^{-1}) was estimated by the following equation:[21]

$$\frac{GPP}{fPAR} = \frac{\alpha \times PAR \times P_{max}}{\sqrt[2]{P_{max}{}^2 + \alpha^2 \times PAR^2}}, \quad \text{(Equation 2)}$$

where PAR is photosynthetically active radiation (MJ m^{-2} 30 min^{-1}) and P_{max} is maximum gross photosynthesis (g C m^{-2} MJ^{-1}). The α and P_{max} were estimated using half-hourly observed GPP and PAR for each day, and the ranges of the estimated α and P_{max} were set as $0 < \alpha < 1$ and $0 < P_{max} < 30$, respectively.

In addition, we also investigated the seasonal changes of photosynthetic capability on a global scale. A global vegetation GPP dataset estimated by the machine-learning model MPI-BGC[34] was used to calculate the LUE by Equation 1 over the extratropical regions across the globe from 1982 to 2011. A global reanalysis dataset, i.e., Modern-Era Retrospective analysis for Research and Applications (MERRA-2), was used to provide global PAR to calculate the global LUE by Equation 1. fPAR was derived from the GIMMS3g NDVI dataset.[33] Further information on the MPI-GBC, MERRA-2, and GIMMS3g NDVI datasets are provided in the following section.

Datasets

In our study, 100 eddy covariance sites with more than 3-year measurements from the FLUXNET2015 dataset: http://www.fluxdata.org were utilized to analyze the differences in VPD and photosynthetic capability. Detailed information on the selected FLUXNET sites is shown in Table S1. Half-hourly data of GPP, PAR, air temperature (T_a), and VPD were collected for 1991–2014. The meteorological variables were gap-filled in both space and time by the marginal distribution sampling method as described in Reichstein et al.[35] and/or downscaled from the ERA-Interim reanalysis dataset.[36] The carbon flux measurements (i.e., net ecosystem exchange [NEE]) were partitioned into GPP and ecosystem respiration (R_e) using a nighttime-based approach.[35]

The newest release of the Advanced Very High Resolution Radiometer (AVHRR) NDVI was used to calculate fPAR by Equation 1 from 1982 to 2015.

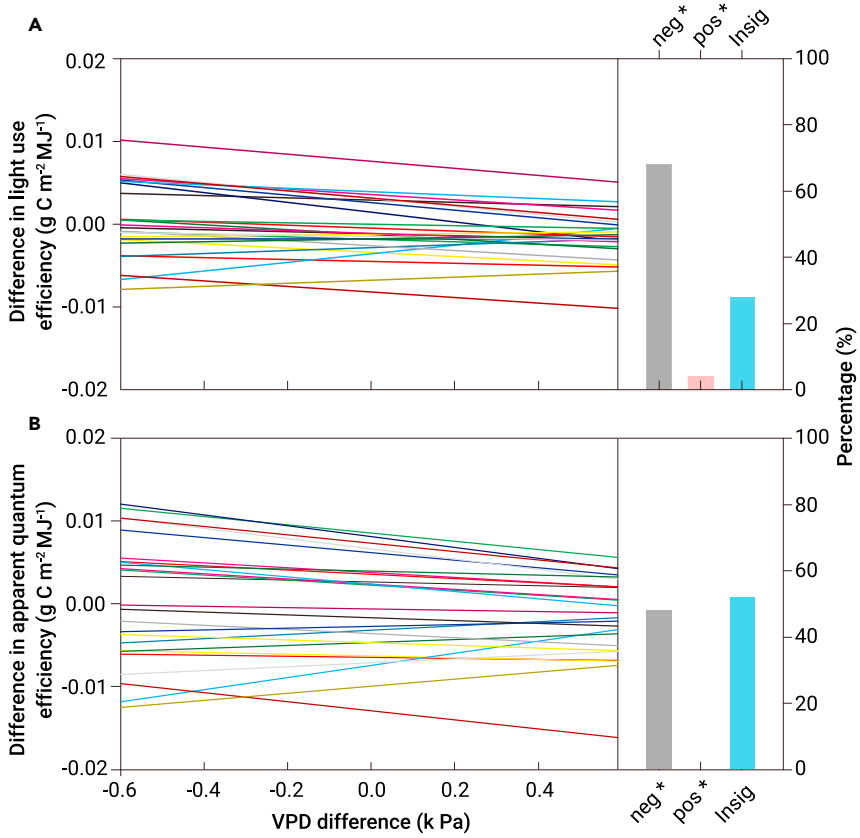

Figure 4. Correlations of averaged vapor pressure deficit (VPD) differences and differences in the photosynthetic parameters between spring and autumn at 25 eddy covariance sites Each color line denotes the linear regression of the mean annual differences in VPD and (A) light use efficiency and (B) apparent quantum efficiency between spring and autumn at each eddy covariance site. Bars show the percentages of significantly ($p < 0.05$) negative correlations (neg*), significantly positive correlations (pos*), and insignificant correlations (Insig), respectively.

The AVHRR is a nonstationary NDVI version 3 dataset produced by the GIMMS3g group.[37] GIMMS3g contains global NDVI observations at approximately 8-km spatial resolution and bimonthly temporal resolution. Each 15-day data measurement is made by maximum value compositing, a process that aims to minimize the influence of atmospheric contamination from aerosols and clouds.

The monthly gridded CRU dataset: http://www.cru.uea.ac.uk/data was used to investigate the seasonal differences in VPD and its long-term changes. The CRU

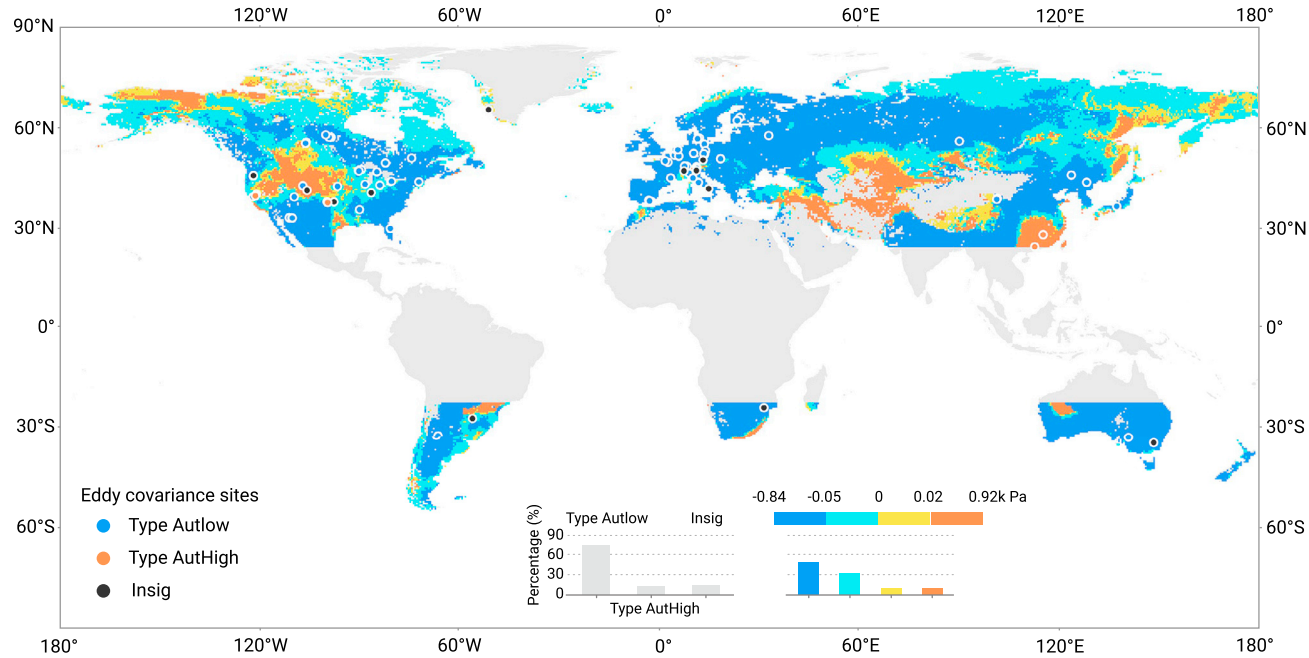

Figure 5. Differences in vapor pressure deficit (VPD) derived from Climate Research Unit (CRU) and eddy covariance towers between autumn and spring at the same air temperature The negative values indicate lower VPD in autumn than in spring and vice versa. Types AutLow and AutHigh denote the sites with VPD significantly ($p < 0.05$) lower and higher in autumn than in spring, respectively. Insig indicates the sites with VPD showing insignificant differences between spring and autumn. Left inset shows the percentages of the AutLow, AutHigh, and Insig sites derived from the CRU dataset, and right inset shows the frequency distributions of the divided four categories of the autumn and spring VPD differences (see legend). Stippling indicates the areas with insignificant seasonal differences in CRU VPD.

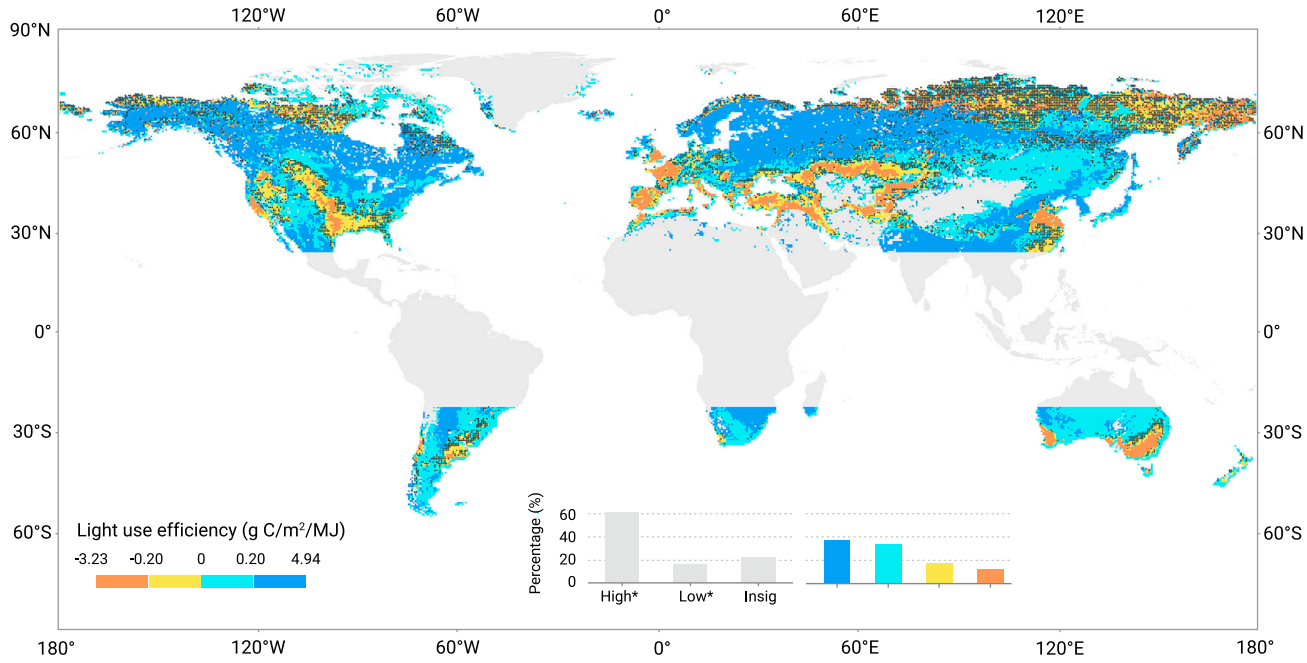

Figure 6. Differences in light use efficiency (LUE) derived from data-driven vegetation gross primary production dataset between autumn and spring at the same air temperature The positive values indicate higher LUE in autumn than in spring and vice versa. Stippling indicates the areas where the spring and autumn LUE differences are not significant. Left inset shows the percentages of the areas with significantly ($p < 0.05$) higher (High*) and lower (Low*) LUE in autumn than in spring, and insignificant differences in LUE between the two seasons (Insig). Right inset shows the frequency distributions of the four divided categories of the spring and autumn LUE differences (see legend).

dataset with spatial resolution of 0.5° × 0.5° was produced on the basis of observations from globally distributed meteorological stations.[38] VPD was then calculated as follows:

$$SVP = 6.112 \times f_w \times e^{\frac{17.67 \times T_a}{T_a + 243.5}}, \quad \text{(Equation 3)}$$

$$f_w = 1 + 7 \times 10^{-4} + 3.46 \times 10^{-6} \times P_{mst}, \quad \text{(Equation 4)}$$

$$P_{mst} = P_{msl} \times \left(\frac{T_a + 273.16}{(T_a + 273.16) + 0.0065 \times Z} \right)^{5.625}, \quad \text{(Equation 5)}$$

$$VPD = SVP - AVP, \quad \text{(Equation 6)}$$

where T_a is the air temperature (°C), Z is the altitude (m), P_{mst} is the air pressure (hPa), and P_{msl} is the air pressure at mean sea level (101.325 kPa). SVP and AVP are saturated and actual vapor pressure (kPa), respectively. In addition, air temperature derived from the CRU dataset was used in this study to investigate the seasonal responses of VPD to air temperature.

The MPI-BGC GPP dataset, with spatial resolution of 0.5° × 0.5°, was generated by a machine-learning algorithm based on a global monitoring network of carbon flux and remote sensing observations.[34] PAR from the MERRA-2 dataset was derived to calculate the global LUE by Equation 1. The MERRA-2 dataset was produced by NASA's Global Modeling and Assimilation Office using an upgraded version of GEOS-5.[39] In addition, a global root-zone soil moisture dataset generated by the Global Land Evaporation Amsterdam Model (GLEAM v3) was applied to compare root-zone soil moisture between spring and autumn for 1980–2017.[40] MODIS land cover type product (MCD12Q1) at 2005 was used to identify the vegetated regions.

Study area

The study area includes the north of the Tropic of Cancer (23°26′N) and the south of the Tropic of Capricorn (23°26′S), mainly over the extratropical vegetated regions across the globe. The tropical region between 23°26′N and 23°26′S with no pronounced weather seasonality was excluded from consideration. In the Northern Hemisphere, the seasons of spring and autumn were defined as March to May (MAM) and September to November (SON), respectively; and the opposite for the Southern Hemisphere, where spring was defined as SON and autumn was defined as MAM, respectively.

Analysis at the eddy covariance sites

Daily VPD and photosynthetic parameters (i.e., LUE and α) were estimated for the two seasons of spring and autumn over the 100 eddy covariance sites. Considering the temperature strongly regulated VPD and plant photosynthetic capability, we first binned all observations at the same temperature intervals and examined their differences using the paired t test method in order to exclude the effects of temperature. We binned all parameters into different air temperature ranges from 0°C to 29°C (the maximum air temperature for the spring and autumn seasons) at 1°C intervals. The means of VPD, LUE, and α were calculated at each temperature range for spring (Y_{spr}), autumn (Y_{aut}), and both seasons (Y_{mean}), respectively. Due to large differences in the magnitude of VPD, LUE, and α among the investigated sites, one cannot compare the differences in the mean values of Y_{spr} and Y_{aut}. Therefore, the ratios between Y_{spr} (or Y_{aut}) and Y_{mean}, i.e. Y/Y_{mean}, were then compared in the divided temperature ranges from 0°C to 29°C over the 80 AutLow and six AutHigh types of sites, respectively, using the paired t test method.

In addition, the differences between Y_{spr} and Y_{aut} for VPD and two variables of photosynthetic capability were examined using the paired t test method at each individual site. Note that for each site only the temperature ranges with data of the parameters available in both seasons were retained for comparisons.

Analysis over the global scale

The monthly CRU dataset was used to analyze the differences of VPD between spring and autumn at the same air temperature. At each pixel, we first calculated the mean air temperature over all six months of spring and autumn (T_m). The target two months with mean air temperature below and above T_m were then identified for spring and autumn, respectively. VPD in spring (VPD_{spr}) and autumn (VPD_{aut}) at the same air temperature of T_m were determined using the linear relationships in VPD and air temperature between the target two months in spring and autumn, respectively (Figure S3). The same method was used to examine the spring and autumn differences in PAR, LUE, and soil moisture at the global scale.

REFERENCES

1. Yuan, W., Piao, S., Qin, D., et al. (2018). Influence of vegetation growth on the enhanced seasonality of atmospheric CO_2. Glob. Biogeochem. Cycles ***32***, 32–41.
2. Graven, H.D., Keenan, R.F., Piper, S.C., et al. (2013). Enhanced seasonal exchange of CO_2 by northern ecosystems since 1960. Science ***341***, 1085–1089.
3. Chen, J.M. (2021). Carbon neutrality: toward a sustainable future. Innovation **2**, 100127. https://doi.org/10.1016/j.xinn.2021.100127.
4. Tanja, S., Berninger, F., Vesala, T., et al. (2003). Air temperature triggers the recovery of evergreen boreal forest photosynthesis in spring. Glob. Chang. Biol. ***9***, 1410–1426.
5. Richardson, A.D., Hollinger, D.Y., Dail, D.B., et al. (2009). Influence of spring phenology on seasonal and annual carbon balance in two contrasting New England forests. Tree Physiol. ***29***, 321–331.

6. Niu, S.L., Luo, Y.Q., Fei, S.F., et al. (2011). Seasonal hysteresis of net ecosystem exchange in response to temperature change: patterns and causes. Glob. Chang. Biol. ***17***, 3102–3114.
7. Barichivich, J., Briffa, K.R., Myneni, R.B., et al. (2013). Large-scale variations in the vegetation growing season and annual cycle of atmospheric CO_2 at high northern latitudes from 1950 to 2011. Glob. Chang. Biol. ***19***, 3167–3183.
8. Jeong, S.J., Schimel, D., Frankenberg, C., et al. (2017). Application of satellite solar-induced chlorophyll fluorescence to understanding large-scale variations in vegetation phenology and function over northern high latitude forests. Remote Sens. Environ. ***190***, 178–187.
9. Garonna, I., Jong, R., Wit, A.J., et al. (2014). Strong contribution of autumn phenology to changes in satellite-derived growing season length estimates across Europe (1982-2011). Glob. Chang. Biol. ***20***, 3457–3470.
10. Huang, M.T., Piao, S.L., Janssens, I.A., et al. (2017). Velocity of change in vegetation productivity over northern high latitudes. Nat. Ecol. Evol. ***1***, 1649–1654.
11. Fu, Y.S., Piao, S.L., Delpierre, N., et al. (2018). Larger temperature response of autumn leaf senescence than spring leaf-out phenology. Glob. Chang. Biol. ***24***, 2159–2168.
12. Keenan, T.F., Gray, J., Friedl, M.A., et al. (2014). Net carbon uptake has increased through warming-induced changes in temperate forest phenology. Nat. Clim. Chang. ***4***, 598–604.
13. Chapin, F.S., Matson, P.A., and Mooney, H.A. (2011). Principles of Terrestrial Ecosystem Ecology (Springer).
14. Zhang, H.C., Yuan, W.P., Liu, S.G., et al. (2015). Divergent responses of leaf phenology to changing temperature among plant species and geographical regions. Ecosphere ***6***, 250. https://doi.org/10.1890/ES15-00223.1.
15. Yuan, W.P., Luo, Y.Q., Liang, S.L., et al. (2011). Thermal adaptation of net ecosystem exchange. Biogeosciences ***8***, 1453–1463.
16. Farquhar, G.D., and Roderick, M.L. (2003). Pinatubo, diffuse light, and the carbon cycle. Science ***299***, 1997–1998.
17. Novick, K.A., Ficklin, D.L., Stoy, P.C., et al. (2016). The increasing importance of atmospheric demand for ecosystem water and carbon fluxes. Nat. Clim. Chang. ***6***, 1023–1027.
18. Yuan, W.P., Zheng, Y., Piao, S.L., et al. (2019). Increased atmospheric vapor pressure deficit reduces global vegetation growth. Sci. Adv. ***5***, eaax1396.
19. Grossiord, C., Buckley, T.N., Cernusak, L.A., et al. (2020). Plant responses to rising vapor pressure deficit. New Phytol. ***226***, 1550–1566.
20. Xia, J.Y., Chen, J.Q., Piao, S.L., et al. (2014). Terrestrial carbon cycle affected by non-uniform climate warming. Nat. Geosci. ***7***, 173–180.
21. Tenhunen, J.D., Hesketh, J.D., and Gates, D.M. (1980). Leaf photosynthesis models. In Predicting Photosynthesis for Ecosystem Models, J.D. Hesketh and J.W. Jones, eds. (CRC Press), pp. 123–181.
22. Yuan, W.P., Piao, S.L., Qin, D.H., et al. (2018). Influence of vegetation growth on the enhanced seasonality of atmospheric CO_2. Glob. Biogeochem. Cycles ***32***, 32–41.
23. Mott, K., and Parkhurst, D.F. (1991). Stomatal response to humidity in air and helox. Plant Cell Environ. ***14***, 509–515.
24. Buckley, T.N., John, G.P., Scoffoni, C., et al. (2017). The sites of evaporation within leaves. Plant Physiol. ***173***, 1763–1782.
25. Flexas, J., Barbour, M.M., Brendel, O., et al. (2012). Mesophyll diffusion conductance to CO_2: an unappreciated central player in photosynthesis. Plant Sci. ***193***, 70–84.
26. Konings, A.G., Williams, A.P., and Gentine, P. (2017). Sensitivity of grassland productivity to aridity controlled by stomatal and xylem regulation. Nat. Geosci. ***10***, 284–288.
27. Chen, Y., Xia, J.Z., Liang, S.L., et al. (2014). Comparison of evapotranspiration models over terrestrial ecosystem in China. Remote Sens. Environ. ***140***, 279–293.
28. Tiam, S.F., and Yasunari, T. (1998). Climatological aspects and mechanism of spring persistent rains over central China. J. Meteorol. Soc. Jpn. ***76***, 57–71.
29. Maherali, H., Pockman, W.T., and Jackson, R.B. (2004). Adaptive variation in the vulnerability of woody plants to xylem cavitation. Ecology ***85***, 2184–2199.
30. Choat, B., Jansen, S., Brodribb, T., et al. (2012). Global convergence in the vulnerability of forests to drought. Nature ***491***, 752–755.
31. Fontes, C.G., Fine, P., Wittmann, F., et al. (2020). Convergent evolution of tree hydraulic traits in Amazonian habitats: implications for community assemblage and vulnerability to drought. New Phytol. ***228***, 106–120.
32. Novick, K.A., Ficklin, D.L., Stoy, P.C., et al. (2016). The increasing importance of atmospheric demand for ecosystem water and carbon fluxes. Nat. Clim. Chang. ***6***, 1023–1027.
33. Sims, D.A., Rahman, A.F., Cordova, V.D., et al. (2005). Midday values of gross CO_2 flux and light use efficiency during satellite over passes can be used to directly estimate eight-day mean flux. Agric. For. Meteorol. ***131***, 1–12.
34. Jung, M., Reichstein, M., and Bondeau, A. (2009). Towards global empirical upscaling of FLUXNET eddy covariance observations: validation of a model tree ensemble approach using a biosphere model. Biogeosciences ***6***, 2001–2013.
35. Reichstein, M., Falge, E., Baldocchi, D., et al. (2005). On the separation of net ecosystem exchange into assimilation and ecosystem respiration: review and improved algorithm. Glob. Chang. Biol. ***11***, 1424–1439.
36. Vuichard, N., and Papale, D. (2015). Filling the gaps in meteorological continuous data measured at FLUXNET sites with ERA-Interim reanalysis. Earth Syst. Sci. Data ***7***, 157–171.
37. Pinzon, J.E., and Tucker, C.J. (2014). A non-stationary 1981-2012 AVHRR NDVI3g time series. Remote Sens. ***6***, 6929–6960.
38. Harris, I., Jones, P.D., Osborn, et al. (2014). Updated high-resolution grids of monthly climatic observations-The CRU TS3.10 dataset. Int. J. Climatol. ***34***, 623–642.
39. Rienecker, M.M., Suarez, M.J., Gelaro, R., et al. (2011). MERRA: NASA's modern-era retrospective analysis for research and applications. J. Clim. ***24***, 3624–3648.
40. Martens, B., Miralles, D.G., Lievens, H., et al. (2017). GLEAM v3: satellite-based land evaporation and root-zone soil moisture. Geosci. Model Dev. ***10***, 1903–1925.

ACKNOWLEDGMENTS

This study was supported by the National Science Fund for Distinguished Young Scholars (41925001), National Youth Top-notch Talent Support Program (2015-48), Changjiang Young Scholars Programme of China (Q2016161), Fundamental Research Funds for the Central Universities (19lgjc02), and the National Natural Science Foundation of China (41971018 and 31930072).

AUTHOR CONTRIBUTIONS

W.Y. and Y.W. designed the research; W.Y., W.X., Y.W., and X.C. performed the analysis; W.Y. and Y.W. drafted the paper; W.X., X.C., B.Z., L.F., B.H., Z.H., S.L., W.L., and S.P. contributed to interpretation of the results and writing of the paper.

DECLARATION OF INTERESTS

The authors declare no competing interests.

SUPPLEMENTAL INFORMATION

Supplemental information can be found online at https://doi.org/10.1016/j.xinn.2021.100163.

LEAD CONTACT WEBSITE

https://atmos.sysu.edu.cn/teacher/358.